


# Direct Binding to NLRP3 Pyrin Domain as a Novel Strategy to Prevent NLRP3-Driven Inflammation and Gouty Arthritis

Gabsik Yang,<sup>1</sup> Hye E. Lee,<sup>1</sup> Su-Jin Moon,<sup>2</sup> Kyung M. Ko,<sup>3</sup> Jung H. Koh,<sup>3</sup> Jin K. Seok,<sup>1</sup> Jun-Ki Min,<sup>3</sup> Tae-Hwe Heo,<sup>1</sup> Han C. Kang,<sup>1</sup> Yong-Yeon Cho,<sup>1</sup> Hye S. Lee,<sup>1</sup> Katherine A. Fitzgerald,<sup>4</sup> and Joo Y. Lee<sup>1</sup> 

**Objective.** The NLRP3 inflammasome is closely linked to the pathophysiology of a wide range of inflammatory diseases. This study was undertaken to identify small molecules that directly bind to NLRP3 in order to develop pharmacologic interventions for NLRP3-related diseases.

**Methods.** A structure-based virtual screening analysis was performed with ~62,800 compounds to select efficient NLRP3 inhibitors. The production of caspase 1-p10 and interleukin-1 $\beta$  (IL-1 $\beta$ ) was measured by immunoblotting and enzyme-linked immunosorbent assay to examine NLRP3 inflammasome activation. Two gouty arthritis models and an air pouch inflammation model induced by monosodium urate monohydrate (MSU) crystal injection were used for in vivo experiments. Primary synovial fluid cells from gout patients were used to determine the relevance of NLRP3 inflammasome inhibition in human gout.

**Results.** Beta-carotene (provitamin A) suppressed the NLRP3 inflammasome activation induced by various activators, including MSU crystals, in mouse bone marrow–derived primary macrophages ( $P < 0.05$ ). Surface plasmon resonance analysis demonstrated the direct binding of  $\beta$ -carotene to the pyrin domain (PYD) of NLRP3 ( $K_D = 3.41 \times 10^{-6}$ ). Molecular modeling and mutation assays revealed the interaction mode between  $\beta$ -carotene and the NLRP3 PYD. Inflammatory symptoms induced by MSU crystals were attenuated by oral administration of  $\beta$ -carotene in gouty arthritis mouse models ( $P < 0.05$ ), correlating with its suppressive effects on the NLRP3 inflammasome in inflamed tissues. Furthermore,  $\beta$ -carotene reduced IL-1 $\beta$  secretion from human synovial fluid cells isolated from gout patients ( $P < 0.05$ ), showing its inhibitory efficacy in human gout.

**Conclusion.** Our results present  $\beta$ -carotene as a selective and direct inhibitor of NLRP3, and the binding of  $\beta$ -carotene to NLRP3 PYD as a novel pharmacologic strategy to combat NLRP3 inflammasome–driven diseases, including gouty arthritis.

## INTRODUCTION

Inflammasomes are multimolecular assemblies composed of a sensor protein, a caspase, and an adaptor protein, such as an ASC. The NLRP3 inflammasome is the best characterized inflammasome and is well known as playing an essential role in the regulation of immune and inflammatory responses. The NLRP3 inflammasome is activated by a diverse array of pathogen- and danger-associated signals, triggering the formation of a cytoplasmic complex consisting of NLRP3, ASC, and procaspase 1 for

caspase 1 activation, culminating in proteolytic maturation of the proinflammatory cytokines, interleukin-1 $\beta$  (IL-1 $\beta$ ) and IL-18, and in pyroptotic cell death (1).

The NLRP3 inflammasome is closely linked to the initiation and progression of a wide range of inflammatory diseases, thereby highlighting the NLRP3 inflammasome as an efficient therapeutic target (2). NLRP3 inflammasome inhibition can be achieved both indirectly and directly, with indirect inhibition occurring by regulating upstream or downstream signaling events and direct inhibition occurring by targeting NLRP3 inflammasome components. Efforts

Supported by the National Research Foundation of Korea grants NRF-2017R1A2B2006281, NRF-2019R1A2C2085739, NRF-2017R1A4A1015036, and NRF-2020R1A4A2002894 from the Republic of Korea's Ministry of Science, ICT, and Future Planning.

<sup>1</sup>Gabsik Yang, PhD, Hye E. Lee, PhD, Jin K. Seok, PhD, Tae-Hwe Heo, PhD, Han C. Kang, PhD, Yong-Yeon Cho, PhD, Hye S. Lee, PhD, Joo Y. Lee, PhD: College of Pharmacy, The Catholic University of Korea, Bucheon, Republic of Korea; <sup>2</sup>Su-Jin Moon, MD, PhD: St. Mary's Hospital, Uijeongbu, Republic of Korea, and The Catholic University of Korea, Seoul, Republic of Korea; <sup>3</sup>Kyung M. Ko, MD, PhD, Jung H. Koh, MD,

PhD, Jun-Ki Min, MD, PhD: St. Mary's Hospital, Bucheon, Republic of Korea, and The Catholic University of Korea, Seoul, Republic of Korea; <sup>4</sup>Katherine A. Fitzgerald, PhD: University of Massachusetts Medical School, Worcester.

**Drs. Yang and H. E. Lee contributed equally to this work.**

No potential conflicts of interest relevant to this article were reported. Address correspondence to Joo Y. Lee, PhD, Jibong-ro 43, Bucheon, Gyeonggi-do 14662, Republic of Korea. E-mail: joollee@catholic.ac.kr.

Submitted for publication July 29, 2019; accepted in revised form February 27, 2020.

to develop pharmacologic inhibitors of the NLRP3 inflammasome have been reported with sulforaphane,  $\beta$ -hydroxybutyrate, CY-09, and MCC950 (3–6). We first reported directly targeting ASC with a small molecule to inhibit the activation of the NLRP3 inflammasome (7). While searching for inhibitors that directly target the NLRP3 inflammasome, we intended to find small molecules that directly bind to NLRP3.

Upon activation, NLRP3 with a pyrin domain (PYD), a nucleotide-binding and oligomerization (NACHT) domain, and a leucine-rich repeat (LRR) domain, self-oligomerizes and recruits ASC containing a PYD and a caspase recruitment domain (CARD) through PYD–PYD interactions (8) (Supplementary Figure 1A, available on the *Arthritis & Rheumatology* web site at <http://onlinelibrary.wiley.com/doi/10.1002/art.41245/abstract>), inducing a helical assembly of the ASC PYD filaments (9). ASC fibrils form into large ASC speck structures, which recruit procaspase 1 through CARD–CARD interactions, leading to autoproteolytic activation (9–11). We hypothesized that the PYD of NLRP3 would be an efficient target since its inhibition would block the initiation phase of NLRP3 inflammasome activation (Supplementary Figure 1A). To identify novel candidate inhibitors that directly bind to the NLRP3 PYD, we performed a structure-based virtual screening with molecular docking calculations using the NLRP3 PYD structure 3QF2 in the Protein Data Bank (12). The scores of ~62,800 compounds were analyzed with affinity- and efficiency-based metrics, such as binding energy ( $\Delta G$ ) and Glide score (Supplementary Figure 1B). Among the 11 compounds that were chosen for their high *in silico* binding affinity scores and commercial availability,  $\beta$ -carotene was selected for further study in the development of an NLRP3 inhibitor.

## MATERIALS AND METHODS

**Study design.** Our study was designed to examine the efficacy of the NLRP3 inhibitor,  $\beta$ -carotene, in cell systems and animal disease models. Cell studies with mouse primary bone marrow–derived macrophages (BMMs) were performed with at least 3 replicates per experiment, in addition to preliminary optimization studies for dose and time determination. Animal disease models include foot gout, gouty arthritis, and air pouch inflammation relevant to acute gout inflammation. Age-matched mice were randomly grouped for  $\beta$ -carotene or vehicle treatment. Animal numbers for each group or experiment were empirically determined based on pilot studies or previous experiments.

**Human synovial fluid samples.** Synovial fluid was obtained from the knee joints of gout patients with serum uric acid levels of  $>400$   $\mu$ moles/liter and joint effusion. Experiments were approved by the Institutional Review Board (IRB) of human subjects at Bucheon St. Mary's Hospital (no. HC18TESI0098) at The Catholic University of Korea, and were carried out in accor-

dance with IRB guidelines and regulations and the Declaration of Helsinki. Written informed consent was obtained from all patients.

**Animals and cell culture.** Mice (C57BL/6; Orient Bio) were maintained under specific pathogen–free conditions in an animal facility with relative humidity of 40–60% and controlled temperature of 23°C ( $\pm 3^\circ$ C). Animal care and the experimental procedures were conducted under the approval of the Institutional Animal Care and Use Committee (IACUC) of The Catholic University of Korea (permission no. 2014-015). BMMs and 293T cells (human embryonic kidney cells) were prepared and cultured as described previously (13).

**Virtual screening analysis and molecular docking modeling.** For virtual screening, we used the commercially available ZINC natural compounds database (<http://zinc.docking.org/>), which contains more than 6 million compounds in ready-to-dock, 3-dimensional formats. Chemical structures for docking analysis were generated using the LigPrep module in Schrodinger. A crystal structure of the human NLRP3 PYD in the RCSB Protein Data Bank (PDB code: 3QF2) was employed in the docking calculations with the Glide module in the Schrodinger molecular simulation package. After the cocrystal ligand was removed, the resulting structure was used as the receptor model. The structure was subjected to restrained minimization to remove steric clashes by the application of an optimized potential for liquid simulations force field using the Protein Preparation Wizard. The minimization was terminated when the root mean square deviation came to a maximum value of 0.3 Å. The computational docking of all the compounds was performed with the Glide program.

**Immunoblot analysis of inflammasome activation.** BMMs cultured in 6-well plates ( $2 \times 10^6$  cells/ml) were primed with purified lipopolysaccharide (LPS) from *Escherichia coli* (100 ng/ml; List Biological Laboratory) for 4 hours. LPS was washed out with phosphate buffered saline (PBS), and  $\beta$ -carotene (Sigma-Aldrich) was added. After 1 hour, cells were stimulated with the inflammasome activators as follows: 500  $\mu$ g/ml of monosodium urate (MSU) crystals for 4.5 hours, 5 mM of ATP for 1 hour, 10  $\mu$ M of nigericin for 1.5 hours, 1  $\mu$ g/ml of poly(dA–dT) for 5.5 hours, and 10  $\mu$ g/ml of flagellin for 5.5 hours in serum-free medium. Cell lysates were processed for immunoblot assays as previously described (7).

**Enzyme-linked immunosorbent assays (ELISAs).** Cell supernatants were analyzed for IL-1 $\beta$  and IL-18 using specific ELISA kits (R&D Systems), and for IL-1 $\alpha$ , IL-18, IL-6, and keratinocyte chemoattractant (KC), and monocyte chemotactic protein 1 (MCP-1) using a Milliplex MAP Mouse Cytokine/Chemokine Kit (Millipore) (14).

**Surface plasmon resonance (SPR) analysis.** Recombinant PYD protein of NLRP3 was prepared as previously described (12). The PYD protein of NLRP3 was covalently immobilized to a CM5 sensor chip (catalog no. BR-1005-30; GE Healthcare). Beta-carotene cultured in PBS with 0.005% Tween 20 and 5% DMSO was run in the flow cell with a 5  $\mu$ l/minute flow rate at 25°C. The association/dissociation phases were monitored using a Biacore T200 system (GE Healthcare), and the affinity constants were calculated with T200 evaluation software (version 2.0), as described previously (7).

**Transient transfection and luciferase assay.** A pcDNA3.1 nV5-hNLRP3 plasmid was kindly provided by Dr. You-Me Kim (Pohang University of Science and Technology, Pohang, South Korea). ASC- and caspase 1-expression plasmids were generously provided by Dr. Giulio Superti-Furga (Austrian Academy of Sciences, Vienna, Austria) and an iGLuc plasmid was generously provided by Dr. Veit Hornung (University of Bonn, Bonn, Germany). A pCMV-proIL-1 $\beta$  plasmid was obtained from Addgene. Transfection procedure and luciferase assays were performed as previously described (13).

**Immunoprecipitation (IP) and immunoblot assays.** Cell lysates were incubated with an anti-NLRP3 antibody (Adipogen), followed by incubation with Protein A-Sepharose beads (GE Healthcare). Coimmunoprecipitated proteins were processed for immunoblot assays.

**Confocal microscopy analysis.** For confocal microscopy, 293T cells were incubated with an anti-NLRP3 antibody (Adipogen) or an anti-ASC antibody (Santa Cruz Biotechnology), followed by incubation with a secondary antibody, such as an Alexa Fluor 488-conjugated anti-mouse IgG antibody and a fluorescein isothiocyanate-conjugated anti-rabbit IgG antibody. Cells were observed using an LSM 710 confocal microscope (Carl Zeiss AG) (15).

**Air pouch inflammation model.** An air pouch was formed in the back of each 7- to 8- week-old C57BL/6 mouse by subcutaneous injection of sterile air, as previously described (6). On day 4, 0.2 ml of sterilized water containing vehicle (0.02% DMSO) or 30 mg/kg of  $\beta$ -carotene was administered via oral gavage. After 1 hour, 3 mg of MSU crystals suspended in 1 ml of sterile, endotoxin-free PBS was injected into the pouch. Six hours later, the air pouch lavages were collected and processed for ELISAs, immunoblot assays, and histologic analysis (6).

**In vitro caspase 1 activity assay.** Caspase 1 activity was measured with a fluorometric caspase 1 assay kit (Abcam) with recombinant human caspase 1 (BioVision). Fluorescence was measured at 400 nm after 505 nm excitation.

**Myeloperoxidase (MPO) activity assay.** MPO activity was measured with an MPO Colorimetric Activity Assay Kit (BioVision).

**A foot gout model in mice.** For induction of foot gout, 30 mg/kg of  $\beta$ -carotene in 0.2 ml of sterilized water was orally administered to 7- to 8- week-old C57BL/6 mice. As a control, 0.02% DMSO vehicle was used. After 1 hour, either MSU crystals in 2 mg/0.1 ml of sterile, endotoxin-free PBS or PBS alone was administered via subcutaneous injection on the right paw plantar surface (16). Changes in paw thickness were measured for 24 hours. The foot tissues were homogenized in radioimmunoprecipitation assay (RIPA) buffer (50 mM Tris HCl, pH 7.4; 1% NP-40; 0.25% sodium deoxycholate; 150 mM NaCl; 1 mM EGTA; 1 mM PMSF; 1 mM Na<sub>3</sub>VO<sub>4</sub>; 10  $\mu$ g/ml of aprotinin; 10  $\mu$ g/ml of leupeptin), and centrifuged at 12,000 revolutions per minute for 10 minutes. Supernatants were used for MPO assays, ELISAs, immunoblot assays, and histologic analysis (16).

**A gouty arthritis model in mice.** A knee joint gouty arthritis model in mice was performed as previously described (17). For induction of gout, 30 mg/kg of  $\beta$ -carotene in 0.2 ml of sterilized water was orally administered to 7- to 8-week-old C57BL/6 mice. As a control, 0.02% DMSO vehicle was used. After 1 hour, either MSU crystals in 100  $\mu$ g/20  $\mu$ l of PBS or PBS alone was injected into the right knee joint of each mouse. After 24 hours, joint tissue was homogenized in RIPA buffer and centrifuged at 12,000 rpm for 30 minutes. Supernatant was collected for MPO assays and cytokine ELISAs.

**Statistical analysis.** Data are presented as the mean  $\pm$  SEM. Statistically significant differences were analyzed by one-way analysis of variance followed by Duncan's test for multiple comparisons using GraphPad Prism 7.0 (GraphPad). *P* values less than 0.05 were considered significant.

## RESULTS

**Suppression of the NLRP3 inflammasome by  $\beta$ -carotene in BMMs.** We first confirmed the inhibitory effect of  $\beta$ -carotene on the NLRP3 inflammasome in a cell-based system stimulated with representative NLRP3 activators. Beta-carotene suppressed ATP-induced cleavage of procaspase 1 and proIL-1 $\beta$  to caspase 1-p10 and mature IL-1 $\beta$ , respectively, in mouse BMMs, as shown by immunoblotting (Figure 1A). Similarly,  $\beta$ -carotene prevented the production of caspase 1-p10 and IL-1 $\beta$  induced by nigericin or MSU crystals in BMMs (Figure 1A). Consistent with this, secretion of mature IL-1 $\beta$  induced by ATP, nigericin, or MSU crystals was suppressed by  $\beta$ -carotene, as measured by an ELISA of cell culture supernatants (Figure 1B). The results demonstrate that  $\beta$ -carotene suppresses activation of the NLRP3 inflammasome induced by various activators. In contrast,  $\beta$ -carotene

did not inhibit the production of caspase 1 and IL-1 $\beta$  induced by poly(dA-dT) or flagellin in BMMs (Figures 1C and D), showing that  $\beta$ -carotene did not inhibit the activation of AIM2 and NLRC4.

**Direct binding of  $\beta$ -carotene to the PYD of NLRP3.**

ATP, nigericin, and MSU crystals have different activation pathways upstream of NLRP3. The common inhibitory effects of  $\beta$ -carotene on different activators suggest that the target of  $\beta$ -carotene is not signaling molecules or events upstream of NLRP3. Thus, we investigated whether  $\beta$ -carotene directly inhibited the NLRP3 inflammasome complex independently of the activators. NLRP3 inflammasome activation was induced by overexpression of the NLRP3 inflammasome components in 293T cells along with the iGLuc luciferase reporter gene, which responds to inflammasome activation (18). Beta-carotene suppressed the expression of the iGLuc luciferase reporter when 293T cells were transfected with NLRP3, ASC, and caspase 1 (Supplementary Figure 2A, available on the *Arthritis & Rheumatology* web site at <http://onlinelibrary.wiley.com/doi/10.1002/art.41245/abstract>). The results suggest that  $\beta$ -carotene directly inhibits the NLRP3 inflammasome

complex independently of activators. Interestingly,  $\beta$ -carotene was not able to inhibit the expression of the iGLuc luciferase reporter induced by ASC+ caspase 1 or caspase 1 alone in 293T cells (Supplementary Figures 2B and C), suggesting that the inhibitory effect of  $\beta$ -carotene requires the presence of NLRP3.

To investigate whether  $\beta$ -carotene could directly bind to NLRP3, an SPR assay was performed with recombinant human NLRP3 PYD. Beta-carotene directly bound to the PYD of NLRP3, but not to ASC, in a dose-dependent manner (Figure 2A).

Molecular modeling analysis of the crystal structure of dimeric human NLRP3 PYD suggests a docking model between  $\beta$ -carotene and the PYD domain of NLRP3. A single molecule of  $\beta$ -carotene bound to NLRP3 PYD, and the final model contained amino acid residues 5–94 (Figures 2B and C). The electron density of  $\beta$ -carotene was evident in the solved NLRP3 PYD structure, which featured  $\beta$ -carotene on the surface formed by H5 and H6 of NLRP3 PYD (Figures 2B and C). Beta-carotene bound to the hydrophobic groove that was composed of hydrophobic residues, including Ala<sup>69</sup>, Val<sup>72</sup>, Trp<sup>73</sup>, Tyr<sup>84</sup>, and Glu<sup>91</sup>, in H5 and H6 (Figures 2B and C and Supplementary Figure 3A, available

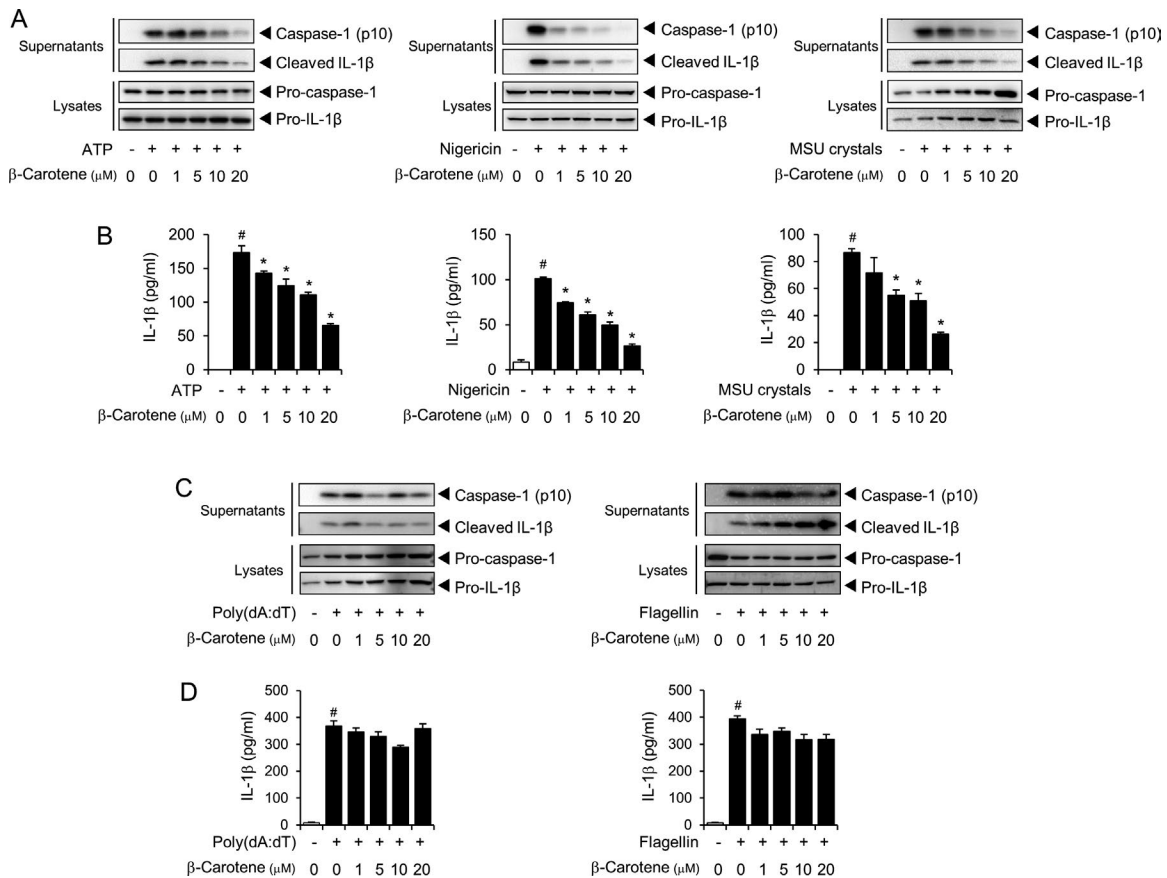


**Figure 1.** Beta-carotene suppression of NLRP3 inflammasome activation. Mouse primary bone marrow-derived macrophages were primed with lipopolysaccharide for 4 hours. Cells were treated with  $\beta$ -carotene for 1 hour and then stimulated with the indicated agonist. **A** and **C**, Cell culture supernatants and cell lysates were immunoblotted for caspase 1-p10, interleukin-1 $\beta$  (IL-1 $\beta$ ), procaspase 1, and proIL-1 $\beta$ . **B** and **D**, Cell culture supernatants were analyzed for secreted IL-1 $\beta$  by enzyme-linked immunosorbent assay. Values are the mean  $\pm$  SEM (n = 3 mice per group). Results are representative of at least 2 independent experiments. # =  $P < 0.05$  versus vehicle alone. \* =  $P < 0.05$  versus ATP, nigericin, or monosodium urate (MSU) crystals alone.

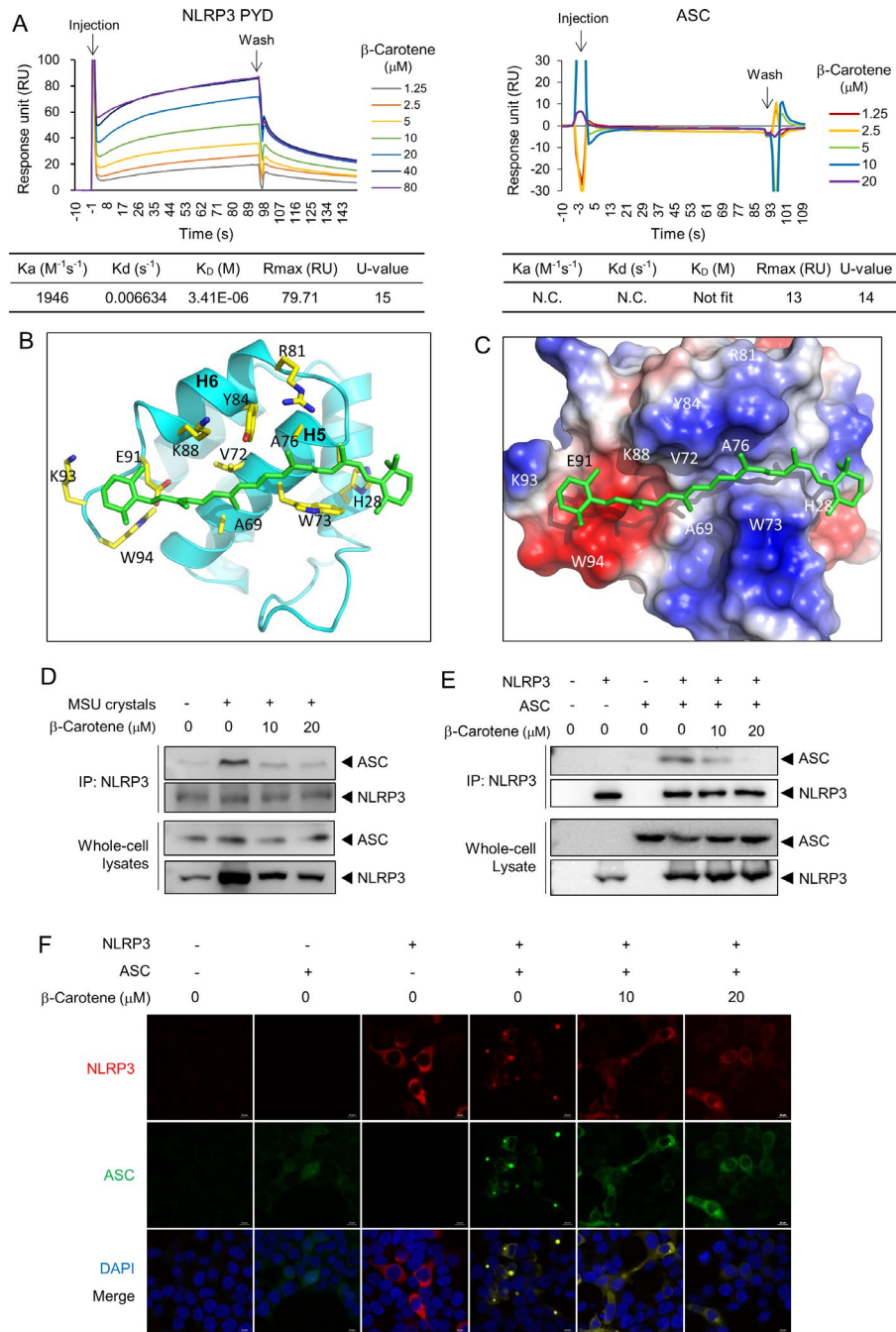


**Figure 2.** Beta-carotene directly binds to the pyrin domain (PYD) of NLRP3. **A**, Sensorgrams of  $\beta$ -carotene binding to the recombinant protein of human NLRP3 PYD or human ASC obtained from surface plasmon resonance (SPR) analysis. Tables show kinetic parameters of the binding between  $\beta$ -carotene and the recombinant proteins. Maximal expected binding level (Rmax) was calculated with Biacore T200 evaluation software. N.C. = not calculated. **B**, Proposed molecular docking model for  $\beta$ -carotene binding to NLRP3 PYD. **C**, Electrostatic surface binding model for  $\beta$ -carotene (green) and NLRP3 PYD, with negative charge (red) and positive charge (blue). **D**, Mouse primary bone marrow-derived macrophages were primed with lipopolysaccharide. Cells were treated with  $\beta$ -carotene for 1 hour and then stimulated with 500  $\mu$ g/ml of monosodium urate (MSU) crystals for 6 hours. Cell lysates were analyzed by immunoprecipitation (IP) with an anti-NLRP3 antibody, followed by immunoblotting as indicated, to demonstrate the association of endogenous NLRP3 and endogenous ASC and the impact of  $\beta$ -carotene on that association. **E**, NLRP3 or ASC expression plasmids were used to transfect 293T cells, and 293T cells were treated with  $\beta$ -carotene for 16 hours. Cell lysates were immunoprecipitated with an anti-NLRP3 antibody, followed by immunoblotting as indicated, to demonstrate the interaction between NLRP3 and ASC induced upon exogenous expression in 293T cells. **F**, NLRP3 or ASC expression plasmids were used to transfect 293T cells, and 293T cells were treated with  $\beta$ -carotene. Cells were stained for NLRP3 (red) and ASC (green). Nuclei were stained with DAPI (blue). Results are representative of at least 2 independent experiments.

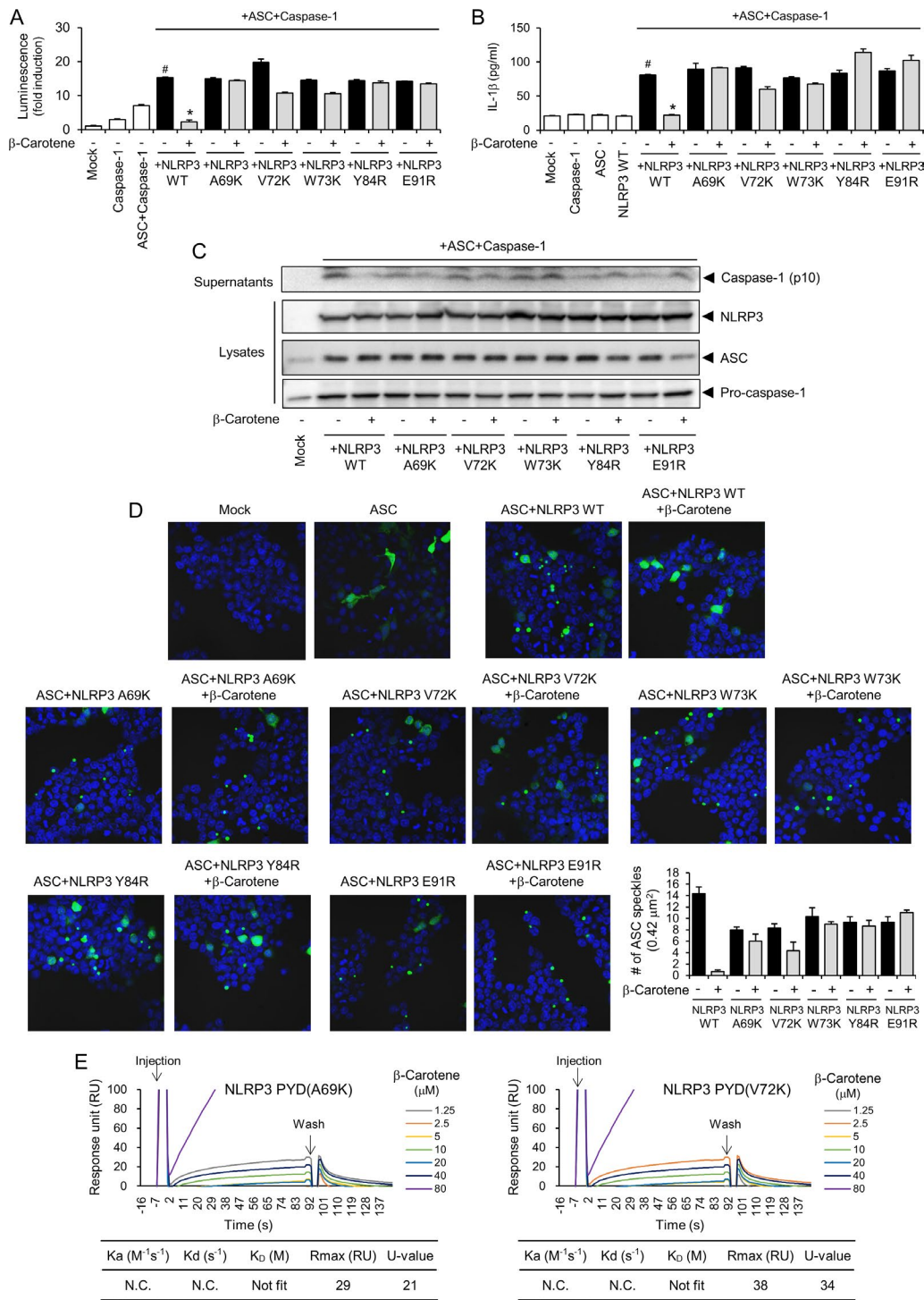


**Figure 3.** Identification of essential amino acids for the interaction between β-carotene and NLRP3 PYD. **A–D**, 293T cells were transiently transfected with expression plasmids of wild-type (WT) NLRP3, NLRP3 mutants, ASC, and caspase 1. The iGLuc luciferase reporter plasmid (**A**) and pro-interleukin-1β (proIL-1β) expression plasmid (**B**) were also transfected. After 8 hours, cells were treated with 20 μM of β-carotene for 16 hours. **A**, Cell lysates were analyzed for luciferase activity derived from iGLuc activation. Activity was normalized to the β-galactosidase activity transfected as an internal control in each sample. **B**, Cell culture supernatants were analyzed for secreted IL-1β by enzyme-linked immunosorbent assay. **C**, Cell culture supernatants and cell lysates were immunoblotted for detection of the indicated molecules. **D**, Cells were stained for ASC (green). Nuclei were stained with DAPI (blue). The bar graph presents the number of ASC speckles formed (n = 3). **E**, Sensorgrams of β-carotene binding to the recombinant protein of the human NLRP3 PYD mutant with A69K or V72K were obtained from SPR analysis as described in Figure 2. In **A**, **B**, and **D**, values are the mean ± SEM (n = 3 mice per group). # = P < 0.05 versus mock alone. \* = P < 0.05 versus NLRP3 WT + ASC + caspase 1 without β-carotene. Results are representative of at least 2 independent experiments. See Figure 2 for other definitions. Color figure can be viewed in the online issue, which is available at <http://onlinelibrary.wiley.com/doi/10.1002/art.41245/abstract>.

on the *Arthritis & Rheumatology* web site at <http://onlinelibrary.wiley.com/doi/10.1002/art.41245/abstract>). NLRP3 associates with ASC through PYD–PYD interactions (19). Molecular modeling suggested that the direct binding of  $\beta$ -carotene to NLRP3 PYD interferes with the interaction between NLRP3 PYD and ASC PYD (Supplementary Figure 3B, <http://onlinelibrary.wiley.com/doi/10.1002/art.41245/abstract>).

Consequently, we next investigated whether  $\beta$ -carotene blocked the association between NLRP3 and ASC using an IP assay with an anti-NLRP3 antibody, followed by immunoblotting with an anti-ASC antibody. MSU crystal stimulation of BMMs resulted in the association of endogenous NLRP3 and endogenous ASC (Figure 2D), while  $\beta$ -carotene prevented the MSU crystal-induced association of NLRP3 and ASC (Figure 2D). Furthermore,  $\beta$ -carotene disrupted the interaction between NLRP3 and ASC induced upon exogenous expression in 293T cells (Figure 2E). These results demonstrate that the binding of  $\beta$ -carotene to the PYD of NLRP3 blocks the assembly of the NLRP3 inflammasome complex.

Since ASC undergoes oligomerization upon association with NLRP3 (20), we further investigated whether the binding of  $\beta$ -carotene to the PYD of NLRP3 affected ASC oligomerization. Confocal microscopy showed that exogenous expression of NLRP3 together with ASC in 293T cells led to speck formation of NLRP3 and ASC as a result of NLRP3 and ASC oligomerization (Figure 2F). In contrast,  $\beta$ -carotene blocked speck formation by NLRP3 and ASC (Figure 2F), demonstrating that  $\beta$ -carotene disrupts the interaction between NLRP3 and ASC.

To confirm the significance of the interaction motif in NLRP3 PYD revealed by molecular docking modeling, we investigated whether mutating the interacting amino acid residues of NLRP3 PYD affected the inhibitory activity of  $\beta$ -carotene. The 5 amino acid residues in NLRP3 that formed the  $\beta$ -carotene binding pocket were mutated to lysine or arginine. Exogenous expression of wild-type (WT) NLRP3 along with ASC, caspase 1, and the iGLuc luciferase reporter in 293T cells resulted in increased luciferase expression, while  $\beta$ -carotene suppressed the luciferase expression induced by the NLRP3 inflammasome (Figure 3A). Exogenous expression of NLRP3 mutants harboring A69K, V72K, W73K, Y84R, or E91R induced luciferase expression to a similar degree as WT NLRP3 (Figure 3A). However,  $\beta$ -carotene failed to suppress the luciferase expression induced by the NLRP3 mutants (Figure 3A).

Reconstitution of WT NLRP3 with ASC and caspase 1 induced an increase in the secretion of IL-1 $\beta$  in 293T cells (Figure 3B).  $\beta$ -Carotene reduced the IL-1 $\beta$  secretion induced by the WT NLRP3 inflammasome (Figure 3B). While reconstitution of NLRP3 mutants with ASC and caspase 1 increased IL-1 $\beta$  secretion to a similar degree as WT NLRP3,  $\beta$ -carotene was not able to block the IL-1 $\beta$  secretion induced by the NLRP3 mutants (Figure 3B). Additionally, exogenous expression of WT NLRP3, ASC, and caspase 1 in 293T cells resulted in the production of cleaved caspase 1 in 293T cells, while  $\beta$ -carotene inhibited the production of cleaved caspase 1 (Figure 3C). The inhibition of the production

of cleaved caspase 1 by  $\beta$ -carotene was not prominent with NLRP3 mutants (Figure 3C).

Furthermore,  $\beta$ -carotene suppressed ASC speck formation in 293T cells transfected with WT NLRP3 and ASC, while ASC speck formation by NLRP3 mutants was not blocked by  $\beta$ -carotene (Figure 3D). Finally, SPR analysis showed that  $\beta$ -carotene did not bind to recombinant human NLRP3 PYD with the A69K or V72K mutation (Figure 3E). The results indicate that the amino acids in NLRP3 PYD are essential for the interaction between  $\beta$ -carotene and NLRP3, confirming the interactive motif suggested by the molecular docking model.

### Prevention of acute gouty arthritis by oral administration of $\beta$ -carotene by blocking NLRP3 inflammasome activation.

We assessed the in vivo suppressive effects of  $\beta$ -carotene on the NLRP3 inflammasome using a mouse air pouch inflammation model. Oral administration of  $\beta$ -carotene abolished the production of caspase 1-p10 and mature IL-1 $\beta$  induced by MSU crystals in air pouch exudates (Supplementary Figure 4A, available on the *Arthritis & Rheumatology* web site at <http://onlinelibrary.wiley.com/doi/10.1002/art.41245/abstract>).  $\beta$ -Carotene reduced caspase 1 activity increased by MSU crystals in air pouch exudates (Supplementary Figure 4B). Oral administration of  $\beta$ -carotene also prevented the MSU crystal-induced release of IL-1 $\beta$  and IL-18 into the air pouch exudates, as measured by ELISA (Supplementary Figure 4C). These results confirm the in vivo suppressive effects of  $\beta$ -carotene on the activation of the NLRP3 inflammasome. Histologic examination and MPO activity showed that neutrophil infiltration in the air pouch tissues and exudates was reduced by  $\beta$ -carotene (Supplementary Figures 4D and E). These results demonstrate the in vivo suppression of NLRP3 inflammasome activation by  $\beta$ -carotene, leading to attenuated in vivo inflammatory responses.

We then investigated whether  $\beta$ -carotene exerted in vivo suppressive activity against NLRP3 inflammasome-related diseases using acute gout mouse models. After mice were orally administered  $\beta$ -carotene, MSU crystals was injected into the hind feet of the mice (Figure 4A). MSU crystal injection led to an increase in paw thickness and neutrophil infiltration in foot tissues, as shown by histologic examination and MPO activity, while  $\beta$ -carotene decreased paw thickness to almost normal levels and blocked MSU crystal-induced recruitment of neutrophils to foot tissues (Figures 4B–E). The results demonstrate that oral administration of  $\beta$ -carotene alleviates the inflammatory symptoms of acute gout in mice. In this experiment,  $\beta$ -carotene prevented MSU crystal-induced production of caspase 1-p10 and IL-1 $\beta$  in mouse foot tissues (Figure 4F). Furthermore,  $\beta$ -carotene reduced caspase 1 activity increased by MSU crystals in foot tissue homogenates (Figure 4G). MSU crystal-induced IL-1 $\beta$  and IL-18 production in foot tissues was decreased by  $\beta$ -carotene (Figure 4H).

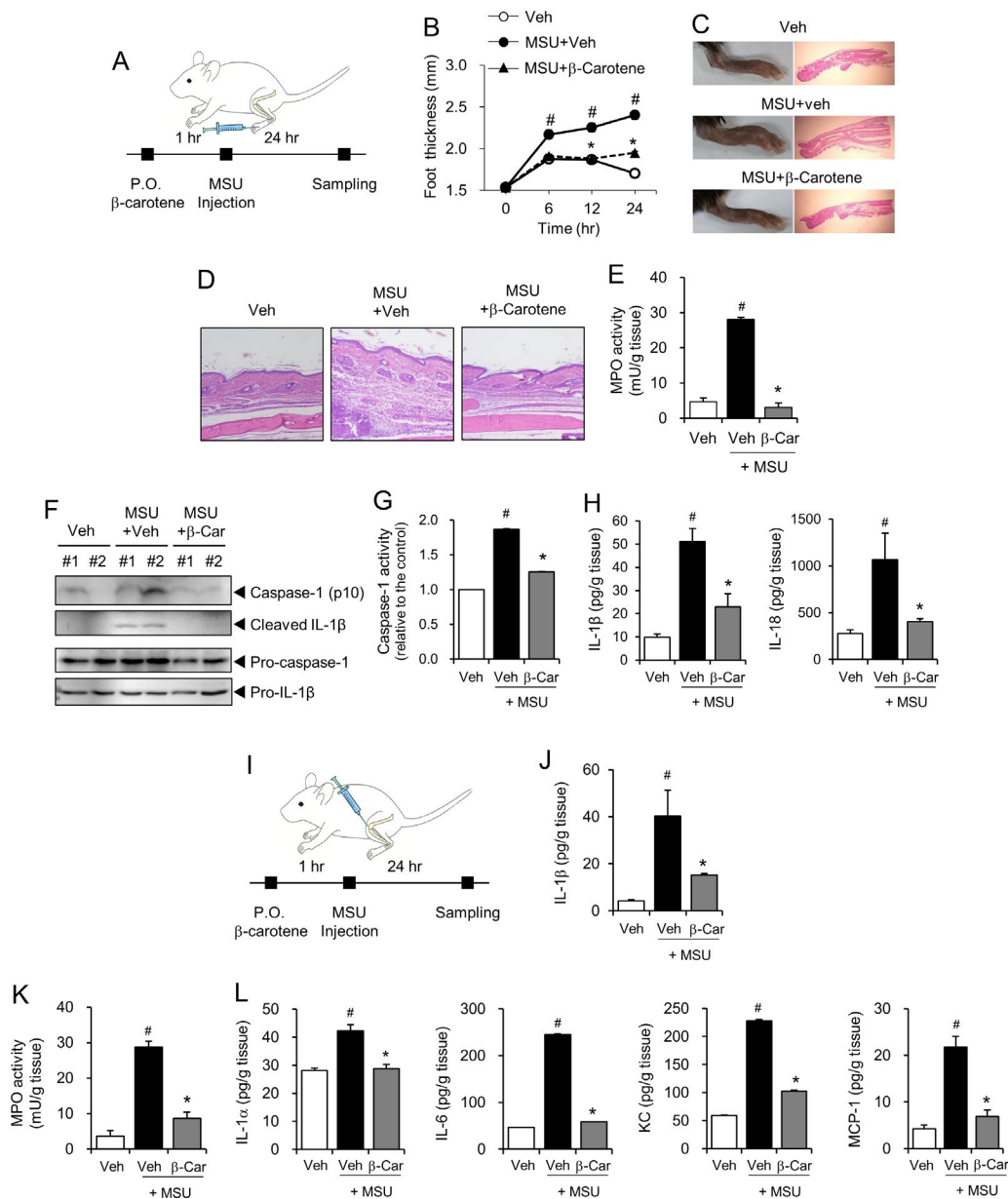


**Figure 4.** Oral administration of  $\beta$ -carotene attenuates in vivo activation of the NLRP3 inflammasome and inflammatory symptoms in acute gout models in mice. **A–H**, Either 30 mg/kg of  $\beta$ -carotene ( $\beta$ -Car) or 0.02% DMSO vehicle (Veh) in water was orally administered (P.O.) in mice. After 1 hour, either monosodium urate (MSU) crystals in 2 mg/0.1 ml of phosphate buffered saline (PBS) or PBS alone was subcutaneously injected into the right hind footpad. After 24 hours, footpad tissues were collected for further analysis. **A**, Experimental scheme. **B**, Time course of paw thickness. **C**, Hematoxylin and eosin (H&E) staining of hind feet. **D**, H&E staining of infiltrated neutrophils. Original magnification  $\times$  400. **E**, Myeloperoxidase (MPO) activity. **F**, Immunoblotting for the indicated molecules in footpad tissue. **G**, Caspase 1 enzyme activity in footpad tissue. **H**, Levels of interleukin-1 $\beta$  (IL-1 $\beta$ ) and IL-18, as measured by enzyme-linked immunosorbent assay (ELISA). **I–L**, Either 30 mg/kg of  $\beta$ -carotene or 0.02% DMSO vehicle in water was orally administered in mice. After 1 hour, either 100  $\mu$ g of MSU crystals in 10  $\mu$ l of PBS or PBS alone was injected into the right knee joint of each mouse. After 24 hours, joint tissue homogenates were prepared for further analysis. **I**, Experimental scheme. **J**, IL-1 $\beta$  levels in the joint tissues of mice, as measured by ELISA. **K**, MPO activity in the joint tissues. **L**, IL-1 $\alpha$ , IL-6, keratinocyte chemoattractant (KC), and monocyte chemoattractant protein 1 (MCP-1) in the joint tissues, as measured by ELISA. Values are the mean  $\pm$  SEM ( $n = 6$  mice per group). # =  $P < 0.05$  versus vehicle. \* =  $P < 0.05$  versus MSU crystals alone. Results are representative of at least 2 independent experiments. Color figure can be viewed in the online issue, which is available at <http://onlinelibrary.wiley.com/doi/10.1002/art.41245/abstract>.

To further investigate whether  $\beta$ -carotene would be effective in the treatment of gouty arthritis, MSU crystals was injected into the knee joints of mice after oral administration of

$\beta$ -carotene (Figure 4I). Beta-carotene prevented the increase of IL-1 $\beta$  induced by MSU crystals in the joint tissues, demonstrating the suppressive effects of  $\beta$ -carotene on the NLRP3



inflammasome in the joint tissues (Figure 4J). Oral administration of  $\beta$ -carotene in mice led to a decrease in MPO activity and inflammatory cytokines and chemokines, such as IL-1 $\alpha$ , IL-6, KC, and MCP-1, in joint tissues injected with MSU crystals (Figures 4K and L). These results show that  $\beta$ -carotene suppresses MSU crystal-induced activation of the NLRP3 inflammasome and subsequent inflammatory symptoms in knee joint tissues. The results demonstrate the *in vivo* suppressive effects of  $\beta$ -carotene on NLRP3-dependent inflammatory responses, correlating well with its inhibition of NLRP3 inflammasome activation in gouty tissues.

**Inhibition of the NLRP3 inflammasome by  $\beta$ -carotene in synovial fluid cells obtained from gout patients.** To examine the efficacy of  $\beta$ -carotene in human cells, synovial fluid cells freshly isolated from the knee joints of gout patients were treated with  $\beta$ -carotene (Figure 5 and Supplementary Figure 5, available on the *Arthritis & Rheumatology* web site at <http://online.library.wiley.com/doi/10.1002/art.41245/abstract>). Production of caspase 1-p10 and mature IL-1 $\beta$  was detected in the culture supernatants of synovial fluid cells obtained from gout patients, while  $\beta$ -carotene treatment reduced the production of caspase 1-p10 and IL-1 $\beta$  (Figure 5A and Supplementary 5A). Consistent with this, IL-1 $\beta$  secretion from synovial fluid cells obtained from gout patients was decreased by  $\beta$ -carotene treatment in a dose-dependent manner (Figure 5B and Supplementary Figure 5B). The results show that  $\beta$ -carotene effectively suppressed the activation of the NLRP3 inflammasome and the secretion of mature IL-1 $\beta$  in the synovial fluid cells of gout patients, suggesting its efficacy in inhibiting NLRP3 inflammasome-mediated inflammation in human subjects.

## DISCUSSION

To the best of our knowledge, this is the first study to present a direct binding antagonist for the PYD of NLRP3. Our results show that  $\beta$ -carotene directly binds to the PYD of NLRP3, thereby blocking the association between NLRP3 with ASC, and ultimately suppressing NLRP3 inflammasome activation. We provide the interaction motif for the binding of  $\beta$ -carotene to NLRP3 PYD, suggesting a new inhibitory platform for future antagonist development. Our study suggests that the PYD of NLRP3 could be an efficient target in the screening of drug candidates for the treatment of NLRP3-related diseases. Our findings further demonstrate a novel strategy to regulate the activity of the NLRP3 inflammasome and the pathology of related chronic diseases.

The NLRP3 inflammasome is composed of 3 domains: an LRR domain, a NACHT domain, and a PYD. The LRR domain is located at the carboxy terminal and recognizes microbial ligands and endogenous danger molecules. The NACHT domain comprises Walker A and Walker B motifs to exert ATPase activity and participates in the oligomerization of the NLRP3 inflammasome. The PYD domain at the amino-terminal is critical to associate with ASC via ASC via PYD–PYD interactions (21). There are some recent studies regarding inhibitors binding to NLRP3. CY-09 was reported to act as a direct inhibitor of NLRP3, thus enabling NLRP3 to bind to the Walker A motif of the NACHT domain, and thereby interfering with ATP binding to NLRP3 (5). Oridonin covalently binds to the cysteine 279 of NACHT domain, interrupting NLRP3 to interact with NEK7 (22). MCC950 was shown to directly bind to the Walker B motif to block ATPase activity (23). Trani-last directly binds to the NACHT domain to inhibit NLRP3–NLRP3 interaction via an ATPase-independent manner (24). Additionally, OLT1177 inhibits ATPase activity of the NLRP3, suggesting its

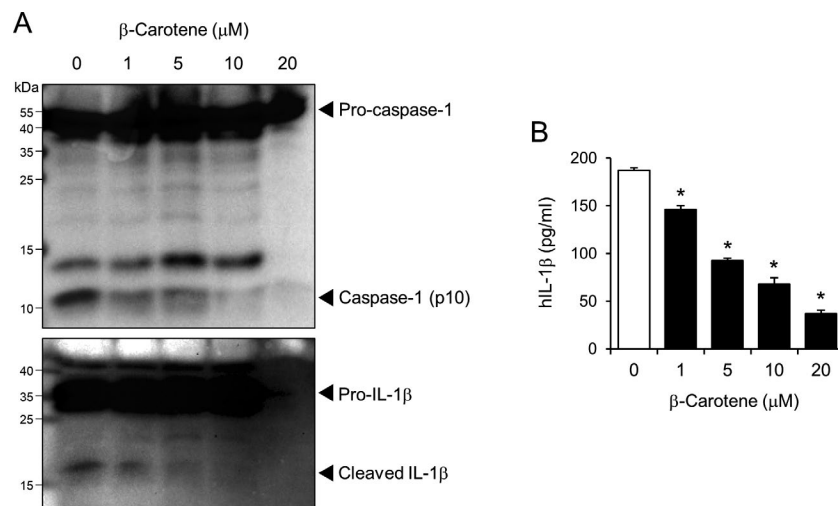


**Figure 5.** Efficacy of  $\beta$ -carotene in the suppression of the NLRP3 inflammasome in primary synovial fluid cells from a gout patient. Primary synovial fluid cells were isolated from a gout patient and treated with various doses of  $\beta$ -carotene for 16 hours. **A**, Levels of procaspase 1, caspase 1-p10, pro-interleukin-1 $\beta$  (proIL-1 $\beta$ ), and IL-1 $\beta$  were analyzed by immunoblotting. **B**, Human IL-1 $\beta$  (hIL-1 $\beta$ ) was assessed in cell supernatants using enzyme-linked immunosorbent assay. Values are the mean  $\pm$  SEM of 5 separate assays run on the sample from 1 gout patient, at each dose of  $\beta$ -carotene. \* =  $P < 0.05$  versus group that received vehicle alone.

binding to NLRP3 (25). Mostly, these inhibitors target the NACHT domain of the NLRP3, resulting in the suppression of ATPase activity, while inhibitors targeting the PYD domain have been rarely studied. Therefore, our study provides a novel inhibitory method to suppress the NLRP3 inflammasome by directly binding to its PYD domain.

Beta-carotene is also called plant-derived provitamin A, yielding 2 molecules of vitamin A (retinol) by  $\beta$ -carotene 15, 15'-monooxygenase in the intestinal mucosa (26). Although the antioxidant activity of  $\beta$ -carotene is widely reported, our study is the first to reveal a novel mechanism by which  $\beta$ -carotene exerts antiinflammatory activity and regulates immune responses. The results of our study demonstrate that  $\beta$ -carotene effectively prevents NLRP3 inflammasome activation, linking to in vivo inhibitory efficacy for NLRP3-driven diseases such as gout. Our findings corroborate with results from an epidemiologic study of a population in the US (27), which demonstrated that there is an inverse association between serum uric acid level and serum  $\beta$ -carotene level and that the intake of  $\beta$ -carotene may be beneficial in protecting against hyperglycemia and gout. Our findings suggest that pharmacologic application of  $\beta$ -carotene could improve inflammatory symptoms related to the NLRP3 inflammasome, such as gout. In future studies, the application of  $\beta$ -carotene could be expanded to other diseases related to NLRP3 inflammasome-mediated autoinflammation (e.g., adult-onset Still's disease, juvenile idiopathic arthritis, and Behçet's disease) (28).

In healthy subjects, basal serum  $\beta$ -carotene levels are  $<1$   $\mu\text{moles/liter}$ . However, several intervention studies have shown the eminent elevation of serum  $\beta$ -carotene levels after supplementation of  $\beta$ -carotene. Micozzi et al reported that continuous intake of 30 mg of  $\beta$ -carotene each day for 6 weeks increased plasma  $\beta$ -carotene levels in healthy men from  $0.303 \pm 0.130$   $\mu\text{moles/liter}$  at baseline to  $7.901 \pm 1.381$   $\mu\text{moles/liter}$  (29). The Carotene and Retinol Efficacy Trial showed that the intake of 30 mg of  $\beta$ -carotene each day for 10 months resulted in a marked increase in serum  $\beta$ -carotene levels from a mean 0.13  $\mu\text{moles/liter}$  to 3.75  $\mu\text{moles/liter}$  (30). In the Carotene Prevention Trial, with the supplementation of 50 mg of  $\beta$ -carotene each day, plasma  $\beta$ -carotene concentrations increased by 9–10-fold throughout the 60 month study period with a median of 0.225  $\mu\text{moles/liter}$  (interquartile range [IQR] 0.125–0.355) at baseline to 2.255  $\mu\text{moles/liter}$  (IQR 1.170–4.395) at 3 months, 3.015  $\mu\text{moles/liter}$  (IQR 1.535–5.830) at 48 months, and 2.775  $\mu\text{moles/liter}$  (IQR 1.945–6.320) at 60 months (31). In the Skin Cancer Prevention Study, median plasma  $\beta$ -carotene levels increased from 0.335  $\mu\text{moles/liter}$  at entry to 3.163  $\mu\text{moles/liter}$  in subjects who received a 1-year supplementation of 50 mg of  $\beta$ -carotene per day. Plasma  $\beta$ -carotene concentrations even ranged up to 16.090  $\mu\text{moles/liter}$  (32). These findings suggest that consistent supplementation with  $\beta$ -carotene may lead to the elevation of serum  $\beta$ -carotene levels to inhibitory doses in the 10–20  $\mu\text{moles}$  range.

In summary, the crucial role of the NLRP3 inflammasome in the pathology of acute gout has been confirmed in human studies (33–35). Therefore, our experimental results may further support the clinical relevance of the NLRP3 inflammasome in gout by demonstrating that  $\beta$ -carotene supplementation hampers NLRP3 inflammasome activity and resolves the progression of acute gout. Although further investigation in human subjects is needed to validate the therapeutic significance of our work, we present pivotal evidence that  $\beta$ -carotene acts as an antiinflammatory vitamin that inhibits the NLRP3 inflammasome.

## AUTHOR CONTRIBUTIONS

All authors were involved in drafting the article or revising it critically for important intellectual content, and all authors approved the final version to be published. Dr. Lee had full access to all of the data in the study and takes responsibility for the integrity of the data and the accuracy of the data analysis.

**Study conception and design.** Yang, H. E. Lee, Kang, H. S. Lee, J. Y. Lee.

**Acquisition of data.** Yang, H. E. Lee, Moon, Ko, Koh, Seok, Min, J.Y. Lee.  
**Analysis and interpretation of data.** Yang, H. E. Lee, Heo, Cho, Fitzgerald, J. Y. Lee.

## REFERENCES

1. Franchi L, Munoz-Planillo R, Nunez G. Sensing and reacting to microbes through the inflammasomes. *Nat Immunol* 2012;13:325–32.
2. Mangan MS, Olhava EJ, Roush WR, Seidel HM, Glick GD, Latz E. Targeting the NLRP3 inflammasome in inflammatory diseases [review]. *Nat Rev Drug Discov* 2018;17:588–606.
3. Coll RC, Robertson AA, Chae JJ, Higgins SC, Munoz-Planillo R, Inserra MC, et al. A small-molecule inhibitor of the NLRP3 inflammasome for the treatment of inflammatory diseases. *Nat Med* 2015;21:248–55.
4. Youm YH, Nguyen KY, Grant RW, Goldberg EL, Bodogai M, Kim D, et al. The ketone metabolite  $\beta$ -hydroxybutyrate blocks NLRP3 inflammasome-mediated inflammatory disease. *Nat Med* 2015;21:263–9.
5. Jiang H, He H, Chen Y, Huang W, Cheng J, Ye J, et al. Identification of a selective and direct NLRP3 inhibitor to treat inflammatory disorders. *J Exp Med* 2017;214:3219–38.
6. Yang G, Yeon SH, Lee HE, Kang HC, Cho YY, Lee HS, et al. Suppression of NLRP3 inflammasome by oral treatment with sulfaphane alleviates acute gouty inflammation. *Rheumatology (Oxford)* 2018;57:727–36.
7. Lee HE, Yang G, Kim ND, Jeong S, Jung Y, Choi JY, et al. Targeting ASC in NLRP3 inflammasome by caffeic acid phenethyl ester: a novel strategy to treat acute gout. *Sci Rep* 2016;6:38622.
8. Masumoto J, Taniguchi S, Sagara J. Pyrin N-terminal homology domain- and caspase recruitment domain-dependent oligomerization of ASC. *Biochem Biophys Res Commun* 2001;280:652–5.
9. Lu A, Magupalli VG, Ruan J, Yin Q, Atianand MK, Vos MR, et al. Unified polymerization mechanism for the assembly of ASC-dependent inflammasomes. *Cell* 2014;156:1193–206.
10. Franklin BS, Bossaller L, de Nardo D, Ratter JM, Stutz A, Engels G, et al. The adaptor ASC has extracellular and 'prionoid' activities that propagate inflammation. *Nat Immunol* 2014;15:727–37.
11. Schmidt FI, Lu A, Chen JW, Ruan J, Tang C, Wu H, et al. A single domain antibody fragment that recognizes the adaptor ASC defines

- the role of ASC domains in inflammasome assembly. *J Exp Med* 2016;213:771–90.
12. Bae JY, Park HH. Crystal structure of NALP3 protein pyrin domain (PYD) and its implications in inflammasome assembly. *J Biol Chem* 2011;286:39528–36.
  13. Joung SM, Park ZY, Rani S, Takeuchi O, Akira S, Lee JY. Akt contributes to activation of the TRIF-dependent signaling pathways of TLRs by interacting with TANK-binding kinase 1. *J Immunol* 2011;186:499–507.
  14. Yang G, Lee HE, Shin SW, Um SH, Lee JD, Kim KB, et al. Efficient transdermal delivery of DNA nanostructures alleviates atopic dermatitis symptoms in NC/Nga mice. *Adv Funct Mater* 2018;28:1801918.
  15. Yang G, Lee HE, Yeon SH, Kang HC, Cho YY, Lee HS, et al. Licochalcone A attenuates acne symptoms mediated by suppression of NLRP3 inflammasome. *Phytother Res* 2018;32:2551–9.
  16. Lee HE, Yang G, Park YB, Kang HC, Cho YY, Lee HS, et al. Epigallocatechin-3-gallate prevents acute gout by suppressing NLRP3 inflammasome activation and mitochondrial DNA synthesis. *Molecules* 2019;24:E2138.
  17. Amaral FA, Costa VV, Tavares LD, Sachs D, Coelho FM, Fagundes CT, et al. NLRP3 inflammasome-mediated neutrophil recruitment and hypernociception depend on leukotriene B(4) in a murine model of gout. *Arthritis Rheum* 2012;64:474–84.
  18. Bartok E, Bauernfeind F, Khaminets MG, Jakobs C, Monks B, Fitzgerald KA, et al. iGLuc: a luciferase-based inflammasome and protease activity reporter. *Nat Methods* 2013;10:147–54.
  19. Vajjhala PR, Mirams RE, Hill JM. Multiple binding sites on the pyrin domain of ASC protein allow self-association and interaction with NLRP3 protein. *J Biol Chem* 2012;287:41732–43.
  20. Fernandes-Alnemri T, Wu J, Yu JW, Datta P, Miller B, Jankowski W, et al. The pyroptosome: a supramolecular assembly of ASC dimers mediating inflammatory cell death via caspase-1 activation. *Cell Death Differ* 2007;14:1590–604.
  21. Latz E, Xiao TS, Stutz A. Activation and regulation of the inflammasomes [review]. *Nat Rev Immunol* 2013;13:397–411.
  22. He H, Jiang H, Chen Y, Ye J, Wang A, Wang C, et al. Oridonin is a covalent NLRP3 inhibitor with strong anti-inflammasome activity. *Nat Commun* 2018;9:2550.
  23. Coll RC, Hill JR, Day CJ, Zamoshnikova A, Boucher D, Massey NL, et al. MCC950 directly targets the NLRP3 ATP-hydrolysis motif for inflammasome inhibition. *Nat Chem Biol* 2019;15:556–9.
  24. Huang Y, Jiang H, Chen Y, Wang X, Yang Y, Tao J, et al. Tranilast directly targets NLRP3 to treat inflammasome-driven diseases. *EMBO Mol Med* 2018;10:e8689.
  25. Marchetti C, Swartzwelter B, Gamboni F, Neff CP, Richter K, Azam T, et al. OLT1177, a  $\beta$ -sulfonyl nitrile compound, safe in humans, inhibits the NLRP3 inflammasome and reverses the metabolic cost of inflammation. *Proc Natl Acad Sci U S A* 2018;115:E1530–9.
  26. Stutz H, Bresgen N, Eckl PM. Analytical tools for the analysis of  $\beta$ -carotene and its degradation products. *Free Radic Res* 2015;49:650–80.
  27. Ford ES, Choi HK. Associations between concentrations of uric acid with concentrations of vitamin A and  $\beta$ -carotene among adults in the United States. *Nutr Res* 2013;33:995–1002.
  28. Jesus AA, Goldbach-Mansky R. IL-1 blockade in autoinflammatory syndromes. *Annu Rev Med* 2014;65:223–44.
  29. Micozzi MS, Brown ED, Edwards BK, Bieri JG, Taylor PR, Khashik F, et al. Plasma carotenoid response to chronic intake of selected foods and  $\beta$ -carotene supplements in men. *Am J Clin Nutr* 1992;55:1120–5.
  30. Redlich CA, Chung JS, Cullen MR, Blaner WS, van Bennekum AM, Berglund L. Effect of long-term  $\beta$ -carotene and vitamin A on serum cholesterol and triglyceride levels among participants in the Carotene and Retinol Efficacy Trial (CARET). *Atherosclerosis* 1999;143:427–34.
  31. Mayne ST, Cartmel B, Silva F, Kim CS, Fallon BG, Briskin K, et al. Effect of supplemental  $\beta$ -carotene on plasma concentrations of carotenoids, retinol, and  $\alpha$ -tocopherol in humans. *Am J Clin Nutr* 1998;68:642–7.
  32. Nierenberg DW, Stukel TA, Baron JA, Dain BJ, Greenberg ER, for the Skin Cancer Prevention Study Group. Determinants of increase in plasma concentration of  $\beta$ -carotene after chronic oral supplementation. *Am J Clin Nutr* 1991;53:1443–9.
  33. Wang LF, Ding YJ, Zhao Q, Zhang XL. Investigation on the association between NLRP3 gene polymorphisms and susceptibility to primary gout. *Genet Mol Res* 2015;14:16410–4.
  34. Deng J, Lin W, Chen Y, Wang X, Yin Z, Yao C, et al. rs3806268 of NLRP3 gene polymorphism is associated with the development of primary gout. *Int J Clin Exp Pathol* 2015;8:13747–52.
  35. Meng DM, Zhou YJ, Wang L, Ren W, Cui LL, Han L, et al. Polymorphisms in the NLRP3 gene and risk of primary gouty arthritis. *Mol Med Rep* 2013;7:1761–6.